Coastal Altimetry products in the Strait of Gibraltar

J. Gómez-Enri[1], P. Cipollini[2], M. Passaro[3], S. Vignudelli[4], B. Tejedor[1], J. Coca[1]

Abstract

This paper analyzes the availability and accuracy of coastal altimetry sea level products in the Strait of Gibraltar. All possible repeats of two sections of the Envisat and AltiKa ground-tracks were used in the eastern and western portions of the Strait. For Envisat, along-track sea level anomalies (SLA) at 18-Hz posting rate were computed using ranges from two sources, the official Sensor Geophysical Data Records (SGDR) and the outputs of a coastal waveform retracker, the Adaptive Leading Edge Subwaveform (ALES) retracker; in addition, SLA at 1 Hz were obtained from the Centre for Topographic studies of the Ocean and Hydrosphere (CTOH). For AltiKa, along-track SLA at 40 Hz was also computed both from SGDR and ALES ranges. The Sea State Bias correction was recomputed for the ALES-retracked Envisat SLA. The quality of these altimeter products was validated using two tide gauges located on the southern coast of Spain. For Envisat, the availability of data close to the coast depends crucially on the strategy followed for data screening. Most of the rejected data were due to the radar instrument operating in a low-precision non-ocean mode. We observed an improvement of about 20% in the accuracy of the Envisat SLAs from ALES compared to the standard (SGDR) and the reprocessed CTOH data sets. AltiKa shows higher accuracy, with no significant differences between SGDR and ALES. The use of products from both missions allows longer times series, leading to a better understanding of the hydrodynamic processes in the study area.

Index Terms

Coastal Altimetry, Strait of Gibraltar, retracking, data screening, validation, tide gauge

[1] J. Gómez-Enri, B. Tejedor and J. Coca are with the University of Cadiz, Cadiz, Spain (e-mail: {jesus.gomez, begonia.tejedor, josep.coca}@uca.es).
[2] P. Cipollini is with the National Oceanography Centre, Southampton, U.K. (e-mail: cipo@noc.ac.uk).
[3] M. Passaro is with the Deutsches Geodätisches Forschungsinstitut der Technischen Universität München (DGFI-TUM), Munich, Germany, (e-mail: marcello.passaro@tum.de).
[4] S. Vignudelli is with the Istitute of Biophysics (CNR), Pisa, Italy (e-mail: vignudelli@pi.ibf.cnr.it).

1. INTRODUCTION

Coastal altimetry has become a mature discipline thanks to the effort of many research groups and institutions [1][5]. A global analysis of the sea level variability near the coasts using satellite altimeter data is now a realistic prospect by virtue of the availability of new reprocessed data with higher along-track spatial resolutions and better accuracy. However putting this into effect requires a consistent validation effort.

Reprocessing efforts are targeting the two main factors that compromise the availability and quality of altimeter data near the coasts with respect to open ocean: (i) inaccuracies in the retrieval of geophysical information from the shape of the mean returned waveforms from the reflected surface (this retrieval is normally done by some waveform fitting procedures known as *retracking*); and (ii) a poorer characterization of some of the geophysical corrections applied to the data. Present altimetry missions (Cryosat-2, AltiKa, Jason-2) and near-future ones (Sentinel-3, Jason-3, Sentinel-6/Jason-CS) minimize the impact of these factors on data quality by virtue of state-of-the-art radiometric performance (Cryosat-2, AltiKa, Jason-2), use of the Ka-band that allows smaller footprints (AltiKa), and SAR-mode operation (Cryosat-2 and all future missions). For past missions (ERS-1/2, Topex/Poseidon, Envisat, GFO, Jason-1) more efforts still need to be made in order to include their products in coastal applications and models [2].

A radar altimeter measures the two-way travel time of the emitted / reflected signal / echo and the returned power. The amount of energy received is recorded on-board in a time series called a "waveform". The pulse repetition frequency (PRF) determines the number of waveforms recorded per unit of time. The PRF for Envisat Radar Altimeter 2 (RA-2: one of the instruments used in this work) is 1800 (Individual

[5] Successful initiatives launched in the last decade to improve the retrieval of in-shore altimeter data include PISTACH *(Prototype Innovant de Système de Traitement pour l'Altimétrie Côtière et l'Hydrologie)* funded by CNES (*Centre National d'Études Spatiales*); COASTALT (*Development of Radar Altimetry Data Processing in the Coastal Zone*), eSurge and CP4O (*Cryosat+ Oceans*) supported by the European Space Agency (ESA); and the Spanish-funded ALCOVA (*Coastal Altimetry: Validation of altimeter products near the coast*).

Echoes: IEs) per second, i.e. 1800 Hz. The tracker on-board sums incoherently packets of 100 IEs in order to reduce the Rayleigh noise associated with the signals assuming uncorrelated noise between consecutive waveforms [3]. These averaged 18-Hz waveforms are transmitted to ground for post-processing. The along-track spatial separation between 18-Hz points is about 375 m but the corresponding footprint has a diameter varying from ~1.6 to 10 km depending on sea state [4]. The *retracking* of waveforms over the ocean is made assuming the Brown waveform model [5], [6], and yields three parameters: epoch (t_0), which is used to estimate the satellite's distance to the mean reflected surface (retracked *Range*), the amplitude of the received signal: backscatter coefficient (*sigma0*) related to the wind speed at the sea surface (U_{10}) and significant wave height (*SWH)*. Inaccuracies in the estimates of the retracked *Range* near the coasts are mainly due to contamination of the waveforms [7]. This contamination might be due to the proximity of land [8] or patches of calm water [9], [10]. In any cases, the effect over the waveform is often clearly seen in the trailing and leading edges.

The way in which this contamination affects the *retracking* of the contaminated waveforms, and hence the accuracy of the above mentioned parameters, is still a matter of investigation. Different strategies have been proposed to mitigate these effects. They are summarized in [11]. Amongst the various retrackers proposed, we consider the Adaptive Leading Edge Subwaveform (ALES hereinafter) as this has been validated for both *Range* and *SWH* for different missions (Jason-1, Jason-2, Envisat) in a few locations [11], [12], [13]. ALES belongs to the family of retrackers restricting the fitting only to that part of the waveform containing most of the oceanographic information, i.e. the leading edge [14], [15], [16], [17], [18]. The tail of the waveform, more prone to contamination by bright targets in the footprint area, is not considered in the fitting process. ALES, in particular, is a two-pass retracker: the first pass is focused on the leading edge and gives an initial estimate of the *SWH*; this value is then used to optimize the width of the subwaveform retracked in the second pass. The ALES algorithm is described in [11] and in the same study ALES-derived sea level was validated against tide gauges in Trieste (Northern Adriatic-Italy; for Jason-1/2 and Envisat) and Mossel Bay (South African coast; for Jason-2 and Envisat). Validation

showed clear improvements in terms of both quality and quantity of recovered data w.r.t. levels in the Sensor Geophysical Data Record (SGDR) products, which are based on a conventional Brown-model retracker [5]. ALES has also been validated for *SWH* in the German Bay [12], demonstrating that ALES is also able to increase the precision of the *SWH* estimations compared to the SGDR products, and more recently ALES sea level has been successfully compared with data from the ESA sea level Climate Change Intiative (CCI) and from tide gauges in the Danish Straits to assess the sea level annual cycle with a view to climatic applications [13].

In this work we analyze in detail the availability and accuracy of altimeter-derived sea level data from Envisat RA-2 and AltiKa SARAL (Satellite with ARgos and ALtiKa) in the area of the Strait of Gibraltar. Here, Envisat and AltiKa have one 35-day repetitive descending pass in the eastern side of the strait and one ascending in the western side. We assess the accuracy of sea level altimeter data using the time series of two tide gauges located in the Spanish coast between both passes. We analyze the performance of ALES in comparison with the official SGDR product based on [5]. To do this, we estimate the relative root mean square error between concomitant altimeter and tide gauge data in a few land / ocean transition scenarios along the eastern and western sides of the strait. Section 2 of the paper presents the study area. The data sets used (altimeter, tide gauge and auxiliary data) are illustrated in Section 3. Section 4 describes the methodology adopted to create the time series of sea level anomaly from the altimeter and the tide gauge. Section 5 presents the results both in terms of analysis of the availability of altimeter data, and in terms of their accuracy, i.e. along-track root mean square error between altimeter and tide gauge time series. These results are discussed in Section 6 and conclusions are given in Section 7.

2. STUDY AREA

The Strait of Gibraltar (*SoG*, hereinafter) is between the Iberian Peninsula and northern Africa: [35.75º - 36.20º N] - [–5.90ºW - –5.25ºW] (Figure 1). It is the unique connection between the Atlantic Ocean and the Mediterranean Sea and controls the water exchanges between both water masses. The Algeciras Bay (*alg-Bay*) is located

near latitude 36.2º N, at the northeastern end of the strait. The *SoG* has been thoroughly described in the past from different points of view. [19] and [20] analyzed the surface flux of Atlantic water toward the East being compensated by a western flux of Mediterranean deeper, saltier and warmer water. The seasonal and interannual oscillations of these fluxes [21], [22], [23], [24] (among others) are responsible for a sea level difference observed between the Atlantic and the Mediterranean Sea that might be driven by different forcing mechanisms: tides [25], atmospheric pressure variations [26], steric contributions [27], geostrophic controls inside the strait [28] and winds in the surrounding area [29], [24], [30]. In addition to this quasi-steady two-layer water exchange a mesotidal and semidiurnal tide dynamics is observed [31], [32], [33], [34] [35]. The water flow interaction with the topography (Camarinal Sill) in the western side of the strait under certain hydrographic conditions generates a train of internal waves, which move mainly toward the Mediterranean Sea [36], [37], [38], [39], [40].

From an altimetric point of view [29] and [41] analyzed the sea level difference between the Atlantic Ocean and the Mediterranean Sea near the strait using Topex/Poseidon tracks. However, they only used along-track altimeter data at 1-Hz interval (about 6 km along the ground track) in regions deeper than 1000 m at distances greater than 150 km from the eastern and western sides of the strait. They pointed out the lack of accurate altimeter data for shallower regions. More recently, [42] developed a preliminary analysis on Envisat altimeter data availability and accuracy in the study area.

3. DATA SETS

Two passes of Envisat / AltiKa were available in the study area: a descending and an ascending crossing the eastern / western side of the strait, respectively. These are the only satellites with two repetitive passes inside the limits of the *SoG*. The presence and orientation of these tracks in the *SoG* and their relative vicinity to the tide gauges offers a good opportunity to test the quality of coastal altimetry measurements in different land-to-ocean and ocean-to-land transitions. The minimum distance between the satellite's passes (ascending and descending) and the tide gauges was about 14 km

(Figure 1). We defined three along-track segments of interest: Algeciras Bay (*alg-Bay*: 11.0 km long) and Eastern *SoG* (*E-SoG*: 18.0 km) for the descending pass (#0360) and Western *SoG* (*W-SoG*: 29.0 km) for the ascending (#0831). A high quality altimeter-derived coastal product over those two passes would allow some degree of continuity from the two missions (except of course for the 2.5-year gap between the end of the Envisat phase E2 and the start of AltiKa measurements, as detailed below), leading to a better understanding of the hydrodynamic processes at both sides of the strait, which is the ultimate motivation for the present assessment study.

3.1 Envisat RA-2

ESA's satellite Envisat was launched in March 2002 being in operation about 10 years. The satellite had a sun-synchronous quasi polar orbit with a 35-day repeat cycle (phase E2) that changed to a 30-day orbit in October 2010 until the end of the mission in April 2012 (phase E3). In this work we focused on the first, longer, 35-day repeat cycle. The time period analyzed spanned 8 years from October 2002 (cycle 6) to October 2010 (cycle 93) giving a maximum of 88 cycles. The passes of Envisat RA-2 available in the study area were: descending #0360 (D#0360) crossing the study area at about 10:46 UTC time in the eastern side of the strait and ascending #0831 (A#0831) crossing at about 21:58 UTC time in the western side (Figure 1).

3.1.1 SGDR

In this work, we used 18-Hz data from the latest official SGDR product under Version 2.1 (which accounts for satellite orbit evolution and implements the Ultra Stable Oscillator instrumental correction). The information extracted from the SGDR files were: coordinates (time and measurements position) (18-Hz posting rate), *Orbit altitude* (18 Hz), *Range* (ocean retracker at ku-band based on [5]) (18 Hz), 'range' corrections (1 Hz, linearly interpolated to 18 Hz), 'geophysical' corrections (1 Hz, linearly interpolated to 18 Hz) and the Ku-band waveforms (18 Hz). Sea Level Anomaly (SLA hereinafter) along the two track segments analyzed was obtained as detailed in the next section.

3.1.2 ALES

Along-track retracked *Range*, *SWH* and *sigma0* from the ALES retracker were used to estimate SLA at 18-Hz posting rate. We retracked the waveforms of the two track segments available in the SGDR product in the study area along the analyzed time period.

3.1.3 CTOH

Data from the Centre for Topographic studies of the Ocean and Hydrosphere (http://ctoh.legos.obs-mip.fr/products/alongtrack-data/alongtrack-data/) were obtained from the X-TRACK processor, and were distributed by Aviso (Archiving, Validation, and Interpretation of Satellite Oceanographic). This is a Level 3 product with data availability at approximately every 7 km along the Envisat passes analyzed (1-Hz posting rate). X-TRACK does not retrack the waveforms, but aims at improving the availability and accuracy of sea level measurements in coastal zones through more accurate tidal and atmosphere forcing corrections, data editing and filtering [43], [44].

3.2 AltiKa SARAL

AltiKa is a cooperative mission between the Indian Space Research Organisation (ISRO) and the French National Centre of Space Research (CNES). The descending / ascending passes of Altika's SARAL altimeter cross the study area at about 18:51 / 06:02 UTC time, respectively (Figure 1). Sea level data at 40-Hz posting rate were obtained from the official SGDR product available at the Aviso ftp server: avisoftp.cnes.fr/Niveau0/AVISO/pub/saral/sgdr_t/. The time period was May 2013 - January 2015 (19 cycles). The retracked *Range* available from the SGDR is estimated by a Maximum Likelihood Estimation approach: MLE3 full-waveform fitting algorithm that uses the Brown analytical model [5]. The ALES retracker was also applied to the waveforms to estimate the *Range*.

3.3 In-situ data

Two tide gauges were used for comparison against altimeter data: *Tarifa_ENV* and *Tarifa_ALT* for Envisat / AltiKa, respectively.

3.3.1 Tarifa_ENV

The tide gauge was located in the harbor of Tarifa city: [36.0086º N - –5.6026º W] being in operation from 1943 to 2012 (Figure 1). It recorded water levels at 5-minute interval referred to the Tide Gauge Zero (TGZ) with no activity during two years (1962 and 1990) and in some other sporadic periods of time. It was part of the Spanish Institute of Oceanography (IEO) Network and fulfilled the Global and European Sea Level Observing Systems requirements (GLOSS and EOSS, respectively) [45], [46]. It was part of the Permanent Service for Mean Sea Level (PSMSL) network (http://www.psmsl.org). The measurement system was composed of two instruments: a mechanical float tide gauge and an electromagnetic codifier (Allgomatic data logger) for converting the lineal movement of the wire float to a digital value, with millimeter precision [47].

Figure 2 shows the instantaneous 5-minute water level recorded by the tide gauge (Fig. 2.a) along the time period of comparison against Envisat data (a lack of data was observed between October and December 2002 and in February 2004). A zoom-in between May and July 2007 (Fig. 2.b) clearly shows the semidiurnal tides dominating the signal. The monthly average of the water level (not shown) indicates a clear seasonal cycle in most of the years with an interannual variability.

3.3.2. Tarifa_ALT

The instrument is a MIROS (MIcrowave Remote sensor for the Ocean Surface) radar sensor measuring at 2 Hz located at approximately the same position as *Tarifa_ENV*: [36.0065ºN - –5.6035ºW]. Data are then averaged to 1-minute intervals at the instrument before transmission in real time to a processing facility where a final 5-

minutes product is generated for distribution. Data are available for the period from July 2009 to the present. The tide gauge is managed by the Spanish Puertos del Estado (http://www.puertos.es) and belongs to the Red de Mareógrafos (REDMAR) network of Puertos del Estado. REDMAR is integrated in the PSMSL and GLOSS.

3.4 Auxiliary data

Some of the corrections used to create time series of SLA were applied to both data sources, altimeter and tide gauge: tidal elevation and atmospheric effect.

3.4.1 Tidal model

We used the National Space Institute of Danmarks Tekniske Universitet (DTU) DTU10 global ocean tide model [48]. This is an updated version of the AG95 (Andersen-Grenoble) ocean tide model with a resolution of 0.125º x 0.125º based on the finite element solution, FES2004 [49]. We used the routines provided by DTU to estimate the total geocentric tidal elevation for the time and position of every 18 / 40 Hz Envisat / AltiKa data point along the two tracks. The same routines were used to detide the water level from the tide gauges.

The performance of this model at the *Tarifa_ENV* location was checked. We applied a harmonic analysis to one year (2009) of tide gauge data and obtained the main constituents. We then estimated the in-situ ocean tide (local tide) at the time of the Envisat data at the tide gauge location. The percentage of explained variance by the DTU10 and local tide was calculated as follows [50], [51]:

$$\%\,\mathrm{var} = 100\left(1 - \frac{\sigma^2_{residual}}{\sigma^2_{original}}\right) \quad (1)$$

where σ stands for the standard deviation of the time series, *original* refers to the uncorrected sea level and *residual* refers to the de-tided time series using DTU10 and local tide, respectively. By applying Eq. (1) we found that DTU10 / local tide explain 93% / 95% of the sea level variance in both tracks. We also estimated the root mean square (*rms*) misfit between the main constituents derived from the tide gauge and the

constituents provided by DTU10 as in [52]. The *rms* of the constituents (M_2, S_2, N_2, K_2, K_1, M_4, O_1, P_1 and Q_1) is below 4 cm in all cases with a root square sum (RSS) of 4.6 cm. Thus, DTU10 seems to accurately model the tides in the study area.

3.4.2 Dynamic Atmospheric Correction (DAC)

The altimeter data use a Dynamic Atmospheric Correction (*DAC*) to correct for the effects of high frequency winds and atmospheric pressure oscillations with periods lower than 20 days and the inverted barometer correction [53]. *DAC* is computed with the high-resolution two-dimensional barotropic model MOG2D ("Modèle aux Ondes de Gravité"). The lack of information regarding the winds precluded the estimation of its contributions to the in-situ water level. For this reason we used the regular 6-hourly gridded maps of *DAC* from AVISO to correct these atmospheric effects to the datasets. The correction was estimated interpolating the *DAC* maps to the time series and positions of altimeter and tide gauge data sets.

3.4.3 Mean Sea Surface (MSS)

We used the most updated version of the DTU *MSS*: DTU13 [54], [55]. The spatial resolution is 1 minute by 1 minute. DTU13 was interpolated to the time series of along-track positions of the two tracks of Envisat and AltiKa.

4. METHODOLOGY

From the time series of the tide gauges we extracted the water levels at the two closest times to each altimeter measurement. Tide gauge and altimeter datasets were collocated in time using the satellite measurement as reference interpolating the in-situ water level to the exact time of the radar records. We analyzed the availability of concomitant in-situ and altimeter data. After the collocation we obtained a maximum of 66 / 18 (Envisat / AltiKa) pairs of in-situ and altimeter data along track in D#0360 and 74 / 18 cycles in A#0831. The discrepancy in the number of collocated data in Envisat with respect to the maximum number of cycles (88) was due first, to the unavailability

of in-situ data in some of the dates of the radar measurements and second, to the lack of some altimeter cycles. We computed time series of SLA from altimetry data: Envisat (SGDR - ALES: 18-Hz posting rate, and CTOH: 1 Hz), and AltiKa (SGDR - ALES: 40 Hz). The concomitant time series from the tide gauges were obtained following the posting rates of the altimeter products used. The range and geophysical corrections used from the Envisat SGDR files are provided at 1 Hz so they were linearly interpolated to 18 Hz. In the case of AltiKa, these corrections were available at 40 Hz.

4.1 SLA from altimetry

The SLA was obtained following (2):

$$SLA = Orbit - Range - Range\ Corrections - Geophysical\ Corrections - MSS \quad (2)$$

4.1.1 Orbit

Is the distance between the satellite's orbit and a reference surface: ellipsoid WGS84 for Envisat and the ellipsoid used by the Topex-Poseidon, Jason-1 and 2 missions for AltiKa.

4.1.2 Range

The retracked *Ranges* used in this work for Envisat / AltiKa were: (i) from the ocean retrackers at Ku / Ka bands available in the SGDR products [5] and (ii) from the ALES retracker [11].

4.1.2 Range Corrections

The ionospheric correction applied to Envisat / AltiKa datasets was the Global Ionospheric Maps based on Total Electron Content grids developed by the Jet Propulsion Laboratory. The dry / wet tropospheric corrections applied to both missions

were obtained from the European Centre for Medium Weather Forecast model computed by Météo-France, the French Meteorological Agency.

The Sea State Bias correction (*SSB_SGDR_Env*) applied to Envisat_SGDR was obtained by bilinear interpolations from a look up table which is a function of *SWH* and U_{10} derived from one year of Envisat RA-2 Ku-band waveform retracking [56]. For AltiKa (*SSB_SGDR_Alt*) the same methodology is applied from one year of data. In addition, *SWH* and *sigma0* obtained from Envisat_ALES were used to recompute the *SSB* correction (*SSB_ALES_Env*, hereinafter) for the retracked *Range*. To do this, *sigma0* was converted to U_{10} by using the algorithm described in [57]. Basically, the algorithm uses a first-guess estimation of U_{10} (U_m) obtained by fitting a two segment function (one linear and one exponential) to *sigma0*. *SSB_ALES_Env* was then estimated by bilinear interpolation from the look up table in [56] using *SWH* and U_{10} from ALES as inputs. Note that, as mentioned above, *SSB_SGDR_Env* is interpolated to 18 Hz from the 1-Hz averages; conversely *SSB_ALES_Env* is computed natively at the higher rate so its 18-Hz samples will show high-frequency variability.

4.1.3 Geophysical Corrections

As mentioned, the tidal elevation used was the DTU10 tidal model for both Envisat and AltiKa. Solid Earth Tide and Pole Tide were also added from SGDR. The atmospheric effects were removed by the interpolated *DAC*.

Four time series (at 18 Hz) were obtained for Envisat in the two track segments analyzed: (i) SLA_Envisat_SGDR_{D#0360; A#831} with the *Range* and *SSB_SGDR_Env* coming from the SGDR files based on the Ocean retracker; and (ii) SLA_Envisat_ALES_{D#0360; A#831} with *Range* and *SSB_ALES_Env* obtained from the retracking of the waveforms using the ALES retracker. Two time series (at 1 Hz) were obtained for Envisat CTOH: SLA_Envisat_CTOH_{D#0360; A#831}. Finally, four time series (at 40 Hz) for AltiKa: SLA_AltiKa_SGDR_{D#0360; A#831} and SLA_AltiKa_ALES_{D#0360; A#831}.

A measure of the improvement due to the *SSB_ALES_Env* correction (Envisat data) is the reduction in the uncertainty of the sea level on the two track segments crossing the strait, which we computed as in [58] using the outputs of the ALES retracker. The uncertainty drops from 22.1 and 16.6 cm to 20.8 and 14.2 for D#0360 / A#0831, respectively, when *SSB_ALES_Env* is applied to the SLA_Envisat_ALES instead of the *SSB_SGDR_Env*.

4.2 SLA from tide gauges

With the in-situ time series of water levels interpolated to the exact time of the altimeter measurements of the two passes analyzed (Envisat and AltiKa) we obtained the SLA as:

$$SLA = Water\_Level - Geocentric\ Ocean\ Tide - DAC - MSS \quad (3)$$

- *Water_Level* is the record interpolated to the time of the altimeter measurement.
- *Geocentric Ocean Tide* was extracted from DTU10 global ocean tide model using the location of the tide gauge and the time of the altimeter data as references.
- The atmospheric effects were removed using the interpolated *DAC*.
- *MSS*: is the mean sea level (1990-1999) over the TGZ.

The in-situ time series were: SLA_TG_Envisat_18Hz_{D#0360; A#831} and SLA_TG_Envisat_1Hz_{D#0360; A#831} for comparison against Envisat (18-Hz and 1-Hz products, respectively); and SLA_TG_AltiKa_40Hz_{D#0360; A#831} for AltiKa.

4.3 Root Mean Square Error

The quality of the altimeter SLA time series was made by estimating the relative root mean square error (*rmse*) between the time series of Envisat / AltiKa from both retrackers, and the equivalent time series of the tide gauges. This parameter (also known

as root mean square difference) has been thoroughly used to estimate the validity of coastal altimeter data [11], [59], [60] (and references therein). We performed a relative analysis as no information on the ellipsoidal height of the tide gauges was available. The relative *rmse* was computed removing the temporal mean of the time series before comparison.

5 RESULTS

The results of this study are of two kinds. First, results in terms of data availability (i.e. data quantity) with an analysis of what causes the data dropouts. This is particularly important for Envisat which has chirp bandwidth issues as discussed in Section 5.1 below. Then there are results from the validation against tide gauges, allowing a quantification of the accuracy (i.e. data quality) for oceanographic applications; these are presented in Section 5.2.

5.1 Availability of the coastal altimetry records

Here we analyze the factors affecting the screening out of altimeter data which is necessary before performing the comparison against in-situ data. Three conditions were taken into account for altimeter data rejection: (i) for Envisat RA-2 only, the instrument can be operating in a low-precision, non-ocean chirp bandwidth; (ii) bad quality of the corrections; and (iii) presence of SLA outliers.

5.1.1 *RA-2 chirp bandwidth*

Envisat RA-2 was designed to operate at three different chirp bandwidths in Ku band, depending on the type of surface: 320 MHz (corresponding to a pulse length of 3.125 ns i.e. a resolution of ~47 cm for the single pulse) for ocean zones and 80 or 20 MHz for non-ocean surfaces. In open ocean conditions the waveform shapes have smooth variations over a few seconds hence RA-2 could use the highest resolution without losing tracking of the surface. Over rapidly changing topography (i.e. coastal zones) where the tracking could be lost, the instrument operated in coarser resolutions preventing the interruption of the echo sample collection. The Brown and ALES

retrackers used in this work have so far only been implemented for the ocean-type (320 MHz) waveforms. Thus, only the radar measurements (*Range*) obtained by retracking waveforms with a chirp bandwidth of 320 MHz were taken into account. Measurements taken with lower bandwidths (80 and 20 MHz) have intrinsically much lower precision and resolution (by a factor 4 and 16, respectively) thus making their use not recommended anyway. Figure 3 presents two examples of radargrams showing the waveform shapes (power) along the two tracks segments analyzed: D#0360 (Fig. 3.a) and A#0831 (Fig. 3.c). For the examples we chose orbital cycle number 73 in both cases as the passes in this cycle show all the factors affecting the loss of data identified. We included the corresponding SLA_ALES profiles (Fig. 3.b and 3.d for descending and ascending passes, respectively). The unavailability of radar measurements due to the instrument operating in a non-ocean mode is observed in the northern land-to-ocean transition of D#0360 (20% of waveforms) and the southern transition of A#0831 (30%). In the southern-D#0360 / northern-A#0831 ocean-to-land transitions there is no loss of data as the instrument was operating in ocean mode very close to the land. The radar instrument rapidly changed its chirp bandwidth from 80 to 320 MHz and then back to 80 MHz in this specific cycle in *alg-Bay* (Fig. 3.a). The small width of the bay (~7 km) complicates the interpretation of the 'ocean' waveform shapes due to land contamination in the footprint area.

Figure 4 summarizes the RA-2 data availability considering all the cycles. It shows the number of cycles along the two track segments analyzed having a chirp bandwidth of 320 MHz (black solid line). The number of cycles in 'ocean' mode increases steadily for D#0360 (Fig. 4.a) inside the bay (*alg-Bay*) from the northern land-to-ocean transition to Punta Carnero. Most of the cycles are in this mode in the strait (*E-SoG*) even in the southern part of the track when the satellite approaches its ocean-to-land transition. In ascending track (A#0831) we observe a low number of cycles in ocean mode in the first 10.5 km of the track segment (Fig. 4.b) in the southern land-to-ocean transition. Then, the data availability increases steadily in the second sector of the track (of about 10 km long). Finally, the percentage is almost 100% in a third sector (8.5 km) in the northern track segment.

These results in the *SoG* confirm that for Envisat RA-2 the availability of data in ocean mode (320 MHz) depends significantly on the type of land / ocean transition. In ocean-to-land transitions we observe, on average, a higher number of 'ocean' waveforms than in land-to-ocean transitions. The complex topography of the land makes the radar operate in coarser resolutions in land-to-ocean transitions and it takes some time to switch back to ocean mode. As said, in the remainder of our analysis we only consider data acquired in ocean mode.

5.1.2 Along-track availability of 'range' / 'geophysical' corrections

For any altimeter we expect some loss of data due to poor accuracy of some of the range and geophysical corrections applied to estimate SLA in the vicinity of land, resulting in SLA outliers. To quantify this issue, we determined the number of along-track cycles with corrections inside their validity range. All the corrections used from the SGDR files showed 100% of availability for both passes and both missions. The only exception to this was the *SSB_SGDR_Env/SSB_ALES_Env* for Envisat and *SSB_SGDR_Alt* for AltiKa. This correction is obtained using information gathered from the retracking of the waveforms (*SWH* and U_{10}) [56]. The retrieval of these parameters in the coastal zone might be affected by land reflections in the footprint area. This would in turn lead to inaccurate estimates of SSB. Taking into account the transitions observed in the track segments analyzed, we might expect a number of data rejections due to invalid SSB for both missions. For *SSB_SGDR_Env / SSB_SGDR_Alt* 'invalid' means the values outside the expected range of variation for SSB: [-0.5 - 0] m [61]. For *SSB_ALES_Env*, invalid values were those obtained with *SWH* and U_{10} input values (from ALES retracker) bigger than the upper limits of the look-up-table used (12 m and 20.75 m/s, respectively; the number of invalid values might be reduced with some degree of along-track smoothing of the native 18-Hz *SSB_ALES_Env*, which is scope for future work). For Envisat, the impact of the screening based on the corrections on top of the chirp-based one is shown by the green solid lines in Figure 4. More cycles were lost due to invalid *SSB_SGDR_Env / SSB_ALES_Env* values in *alg-Bay* and at the ocean-to-land / land-to-ocean transitions in the strait. The number of valid cycles increases as the satellite approaches open ocean conditions. For AltiKa, the screening

based on the corrections (not shown) confirms the loss of cycles due to invalid *SSB_SGDR_Alt*.

5.1.3. Removal of SLA outliers

Taking into account only 'ocean' radar measurements and corrections within their range of validity we estimated the time series of SLA (Eq. 2) along the two tracks for both missions. We considered only SLA values within [-1.5 1.5] m. This gave the final number of cycles for comparison against in-situ SLA. The Envisat cycle analyzed in Figure 3 (73) shows the track segments rejected due to: (i) areas where the chirp bandwidth was not 320 MHz; (ii) invalid SSB; and (iii) SLA out of its range of validity (delimited by red arrows in Fig. 3.b and 3.d). The lack of these data is observed in *alg-Bay* and close to the southern ocean-to-land transition in D#0360 (Fig. 3.b). For A#0831 (Fig. 3.d) some data rejection is observed following the land-to-ocean transition, and extends to the first measurements made by the instrument operating in ocean mode.

Figure 4 shows the impact of SLA outlier screening for Envisat as red solid lines. For the sake of comparison amongst retrackers we only considered altimeter time series in locations in which both SGDR-derived and ALES-derived SLAs were available after the screening. A few more cycles are lost in most of *alg-Bay* (Fig. 4.a). The availability of valid data continues increasing in *E-SoG* to reach almost its maximum (66). A small dropout is observed due to the proximity of land as the satellite approaches the southern ocean-to-land transition. Regarding ascending A#0831 (Fig. 4.b) the loss of data due to data screening is only observed in a few locations.

It is interesting to discuss what causes the rejection of so many records in *alg-Bay* (D#0360). The altimeter is in the correct ocean bandwidth mode in more than half of the passes, as in the last few km flown over land before the coastline where the terrain has only moderate slope. However there are difficulties with the corrections especially the SSB as discussed in subsection 5.1.2 above, that result in the rejection of many records. A few more outliers remain in the SLA in the centre of the bay, likely to be a result of the several 'bright targets' (calm water in sheltered areas, see [9])

surrounding it. The corresponding land-to-ocean transition of track A#0831 has a higher proportion (55% to 65% in the first 8 km from the coast) of non-ocean bandwidth records due to the more corrugated terrain over the African coast (the track overflights a 450 m relief at 8 km from the coastline), but a much smaller proportion of rejections due to corrections or SLA outliers.

5.2. Validation of altimeter-derived Sea Level Anomaly

The altimeter data editing generates times series of SLA along the two tracks analyzed. These along-track time series were compared with the concomitant time series of SLA obtained from the tide gauges. Figure 5 shows the time series of SLA tide gauge: SLA_TG_Envisat_18Hz_D#0360 (Fig. 5.a), Envisat descending pass: SLA_Envisat_{SGDR; ALES}_D#0360 (Fig. 5.b), SLA_TG_Envisat_18Hz_A#0831 (Fig. 5.c) and ascending pass: SLA_Envisat_{SGDR; ALES}_A#0831 (Fig. 5.d). We selected the 18-Hz position with the lowest *rmse*. The distance to the nearest tide gauge was about 15 km in both along-track points. The lack of data is mainly observed in the beginning of the time period selected. Tide gauges SLA series ranges between -0.2 and 0.2 m with most of the altimeter SLA values (SGDR and ALES) inside that range. The *rmse* between in-situ and altimeter time series in the along-track points selected was 8 / 10 cm (ALES / SGDR for each track segment).

Figure 6 shows the *rmse* obtained along the two tracks analyzed. We only plotted the results in the along-track positions with at least 20 valid RA-2 cycles. We included the comparison made using the Envisat SLA obtained from CTOH. In general, the along-track *rmse* in #D0360 (Fig. 6.a) ranges between 8 and 40 cm (ALES / SGDR) with the higher values observed in land / ocean transitions (lower number of available cycles). The lower *rmse* are observed at ~14/15 km from the TG location. In this particular track ALES seems to perform better than SGDR in most of the segment. Only two 1-Hz CTOH points were obtained in this track showing similar *rmse* to ALES for the closest CTOH point to the tide gauge position. The *rmse* for #A0831 (Fig. 6.b) ranges between 8 and 50 cm. We observe decreasing values as the track crosses the strait northward. *rmse* is higher in the land / ocean transition. Over this track ALES

performs much better than SGDR in terms of lower *rmse*. Only three 1-Hz CTOH points were obtained for this track with *rmse* values higher than both ALES and SGDR. The improvement of ALES with respect to SGDR confirms previous analysis made in [11].

We included in Figure 6 also the along-track *rmse* using AltiKa, which was screened as per Envisat (except of course for the chirp issue). AltiKa presents a lower *rmse* (below 10 cm) than Envisat, with no difference between the standard (SGDR) and ALES processing. The lack of valid *rmse* was observed in both track segments with higher / lower loss of data in land-to-ocean / ocean-to-land transitions, respectively. The analysis of the retracked *Ranges* obtained with AltiKa (SGDR and ALES) showed unrealistic values in the vicinity of land.

We estimated the mean value of *rmse* (Envisat) in the study area testing the effect of the proximity of land in the calculations. We applied northern and southern land masks of 1 to 5 km from coast before estimating the average of the Envisat *rmse* along the remainder of the track segment. The lack of available Envisat data in most of *alg-Bay* precluded this analysis. The results are summarized in Table 1. ALES gives lower (i.e. better) *rmse* with little dependence on the land mask extent: values with a land mask of 1 km already approach the asymptotic values with a larger land mask.

6. DISCUSSION

The first consideration that needs to be made when discussing the results presented in the previous section is related to the chirp bandwidth. In most of the Envisat cycles for both tracks analyzed the RA-2 instrument was operating in a non-ocean mode when coming out from land and keeping that bandwidth for a few seconds. The overall percentage of non-ocean waveforms is higher than seen in other coastal areas probably due to the complex topography, and conversely in a small number of cycles the chirp bandwidth was found to be 320 MHz even over land: both these phenomena should be investigated further. In summary, the availability of Envisat data amenable to accurate retracking (i.e. with 320 MHz waveforms) is significantly reduced when the chirp 'flag' is taken into account.

The retracking of AltiKa waveforms in the vicinity of land seems to be compromised by the type of transition. Estimates of *Range* using a full-waveform retracker (SGDR) are often wrong especially in land-to-ocean transitions. In some of these cases, even a subwaveform retracker such as ALES is not able to find an estimate of *Range*, due to (i) the retracker failing to find a retrackable subwaveform; or (ii) the subwaveform being too peaky to allow convergence.

The quality of altimeter-derived sea level data in the Strait of Gibraltar depends on many factors: instrument, retracking algorithm, data screening and proximity of the radar measurements of land. AltiKa gives the highest accuracy (in terms of *rmse*) but the data editing already applied to the SGDR precluded any further assessment of this product close to the coast. The quality of the Envisat RA-2 SLA obtained with the ALES retracker is better than the official product (SGDR) and CTOH. The availability of Envisat data in the vicinity of land depends on the type of ocean / land transition with more data in ocean-to-land than land-to-ocean transitions, as previously suggested by [62]. The quality of Envisat data degrades in the last 5 km to the coast, regardless of the type of transition, however along-track *rmse* averages are robust against the inclusion of points up to 1 km to the coast, especially when the ALES retracker is adopted. The *SSB* correction, computed for the first time with *SWH* and U_{10} from ALES (Envisat) improves the quality of the retrieved sea level. This finding reinforces the call for a dedicated sea state bias correction in the coastal zones.

7. SUMMARY AND CONCLUSIONS

In this work we analyzed in detail the Envisat altimeter data availability and accuracy in the Strait of Gibraltar. Sea level anomalies from the official SGDR product and from the ALES retracker were compared against in-situ tide gauge data located at Tarifa harbour, on the Spanish coast. Other reprocessing schemes (CTOH) and satellites (AltiKa) were also considered in this study.

Data screening in the coastal zone is crucial in order to avoid inaccurate altimeter data. We followed three criteria for data rejection:

1. Chirp bandwidth (for Envisat only): the switch to the 'ocean' bandwidth (320 MHz) in land-to-ocean transitions needed a few seconds in most of the cycles analyzed in the Strait of Gibraltar for both track segments. Only the waveforms recorded in ocean mode can be retracked to sufficient precision with the state-of-the-art ocean-oriented retrackers to obtain geophysical information. For this reason most of the nearshore radar measurements must be rejected in this type of transition. The 'ocean' bandwidth is instead kept close to the coast in all the ocean-to-land transitions of the cycles analyzed. We conclude that there is a bias to higher data availability for the ocean-to-land vs. land-to-ocean transition in case of changes in the chirp bandwidth.
2. Along-track availability and quality of the geophysical corrections: the cycle-by-cycle analysis revealed that all the corrections presented full availability along the track segments analyzed. This is mainly due to the fact that most the corrections used are based on models, so no data gaps are expected in the vicinity of the coast. The only exception to this was the sea state bias. This is due to the fact that SSB is linked to the retracking outputs: *SWH* and U_{10}. Any time the estimate of one or both of these two parameters is corrupted the SSB correction will also be affected. We demonstrated, however that SSB recomputation for Envisat using ALES *SWH* and U_{10} yields a better agreement of the SLA with in-situ data.
3. Removal of outliers: the rejection of SLA values outside their range of validity demonstrated that the outliers were mainly confined to the coastal strip in both land-to-ocean and ocean-to-land transitions. In the Algeciras Bay most of the radar measurements were rejected. Two reasons might explain this: (i) The bay is in a land-to-ocean transition and hence a number of measurements are excluded due to the instrument operating in a non-ocean mode (only for Envisat); and (ii) most of the 'ocean' waveforms might still contain land or bright target reflections in the footprint area due to the vicinity of land and calm waters to both sides of the track, and this complicates the retrieval of accurate *Ranges, SWH* and U_{10}.

Overall, the result for the reprocessed ALES Envisat are improved compared to the standard (SGDR) and the reprocessed CTOH data sets. The mean along-track *rmse* in the Strait between ALES and the tide gauge is below 14 / 12 cm (D#0360 / A#0831), which represents about a 20% improvement with respect to the SGDR. The exclusion of nearshore points improved the results slightly (in terms of lower mean along-track *rmse*), mainly for the SGDR product. AltiKa measurements appear to be the most accurate, showing the lowest *rmse* against the tide gauge.

For the first time high-rate SLA data have been derived in the Strait of Gibraltar, the confluence of the Atlantic Ocean and the Mediterranean Sea. The validation of the time series of SLA using ground-truth data has demonstrated that a more accurate *SSB* correction improves the comparison against in-situ data. The availability of data with higher quality will improve the coverage of the coastal zones, especially in challenging areas such as the Strait of Gibraltar. This will also increase their use in many applications, such as long-term coastal sea level changes, storm surges, coastal oceanography, etc. The ability to construct longer time series by using both the Envisat and AltiKa missions (although with an unavoidable 2.5-year gap) paves the way to a better characterization of the oceanic processes.

ACKNOWLEDGMENTS

This work has been partially supported by the ALCOVA Project (CTM2012-37839) funded by the Spanish Ministerio de Economía y Competitividad and FEDER, and by the Spanish Ministerio de Educación, Cultura y Deporte under the "Salvador de Madariaga" Programme. The ALES retracker development has been partially supported by the ESA/DUE eSurge (ESA/ESRIN Contract Number 4000103880/11/I-LG). In-situ data were obtained from the Spanish Institute of Oceanography (IEO). Envisat RA-2 SGDR products were downloaded from ESA Earthnet Online. We are very grateful to Carlos José González-Mejías for his help on the harmonic analysis of the in-situ data.

REFERENCES

[1] S. Vignudelli, A. Kostianoy, P. Cipollini, and J. B. Benveniste (eds.), *Coastal Altimetry*. Berlin, Germany: Springer-Verlag. doi: 10.1007/978-3-642-12796-0, 2011.

[2] F. Birol, and C. Delebecque, "Using high sampling rate (10/20Hz) altimeter data for the observation of coastal surface currents: A case study over the northwestern Mediterranean Sea". *J. Marine Syst.*, doi: 10.1016/j.jmarsys.2013.07.009, 2014.

[3] E. J. Walsh, "Pulse to pulse correlation in satellite radars", *Radio Sci.*, doi: 10.1029/RS017i004p00786, 1982.

[4] D. B. Chelton, J. C. Ries, B. J. Haines, L. L. Fu, and P. S. Callahan, "Satellite altimetry". In L.-L. Fu & A. Cazenave (Eds.), *Satellite Altimetry and Earth Sciences: A Handbook of Techniques and Applications.* San Diego, CA, USA: Academic Press, pp. 1-168, 2001.

[5] G. S. Brown, "The average impulse response of a rough surface and its applications", *IEEE T. Antenn. Propag.,* doi: 10.1109/TAP.1977.1141536, 1977.

[6] G. S. Hayne, "Radar altimeter mean return waveforms from near-normal-incidence ocean surface scattering", *IEEE T. Antenn. Propag.*, doi: 10.1109/TAP.1980.1142398, 1980.

[7] C. P. Gommenginger, P. Thibaut, L. Fenoglio-Marc, G. D. Quartly, X. Deng, J. Gómez-Enri, P. Challenor, and Y. Gao, "Retracking altimeterwaveforms near the coasts - a review of retracking methods and some applications to coastal waveforms". In: Vignudelli, S., Kostianoy, A., Cipollini, P., Benveniste, J. (Eds.), *Coastal Altimetry*. Berlin, Germany: Springer-Verlag, pp. 61-101, 2011.

[8] J. Tournadre, "Signatures of lighthouses, ships, and small islands in altimeter waveforms", *J. Atmos. Ocean. Tech.*, doi: 10.1175/JTECH2030.1, 2007.

[9] J. Gómez-Enri, S. Vignudelli, G. D. Quartly, C. P. Gommenginger, P. Cipollini, P. Challenor, and J. Benveniste, "Modeling Envisat RA-2 waveforms in the Coastal Zone: Case study of calm water contamination". *IEEE Geosc. Rem. Sens. Lettr.*, doi: 10.1109/LGRS.2009.2039193, 2010.

[10] A. Scozzari, J. Gómez-Enri, S. Vignudelli, and F. Soldovieri, "Understanding target-like signals in coastal altimetry: Experimentation of a tomographic imaging technique". *Geophys. Res. Lettr.*, doi: 10.1029/2011GL050237, 2012.

[11] M. Passaro, P. Cipollini, S. Vignudelli, G. D. Quartly, and H. N. Snaith, "ALES: A multi-mission adaptive subwaveform retracker for coastal and open ocean altimetry". *Remote Sens. Environ.*, doi: 10.1016/j.rse.2014.02.008, 2014.

[12] M. Passaro, L. Fenoglio-Marc, and P. Cipollini, "Validation of significant wave height from improved satellite altimetry in the German Bight", *IEEE T. Geosci. Remote*, doi: 10.1109/TGRS.2014.2356331, 2015a.

[13] M. Passaro, P. Cipollini, and J. Benveniste, "Annual sea level variability of the coastal ocean: The Baltic Sea-North Sea transition zone", *J. Geophys. Res.-Oceans*, doi: 10.1002/2014JC010510, 2015b.

[14] J. Y. Guo, X. T. Chang, J. L. Sun, and Y. G. Gao, *Waveform retracking of satellite radar altimeter and applications*. Beijing, China: Surveying and Mapping Press, 186pp, 2013.

[15] N. Idris, and X. Deng, "The retracking technique on multi-peak and quasi-specular waveforms for Jason-1 and Jason-2 missions near the coast", *Mar. Geod.*, doi: 10.1080/01490419.2012.718679, 2012.

[16] F. Mercier, N. Picot, P. Thibaut, A. Cazenave, F. Seyler, P. Kosuth, *et al.,* "CNES/PISTACH project: an innovative approach to get better measurements over inland water bodies from satellite altimetry". Early results EGU General Assembly Conference Abstracts, Vol. 11 (2009), p. 11674

[17] Y. Yang, C. Hwang, H. Hsu, E. Dongchen, and H. Wang, "A subwaveform threshold retracker for ERS-1 altimetry: A case study in the Antarctic Ocean", *Comput. Geosci.*, doi: 10.1016/j.cageo.2011.08017, 2011.

[18] L. Yang, M. Lin, Q. Liu, and D. Pan, "A coastal altimetry retracking strategy based on waveform classification and subwaveform extraction", *Int. J. Remote Sens.*, doi: 10.1080/01431161.2012.701350, 2012.

[19] H. Lacombe, and C. Richez, "The regime in the Strait of Gibraltar". In *Hydrodynamics of Semi-Enclosed Seas*, Jacques C.J. Nihoul (ed.), ISBN: 978-0-444-42077-0, 13-73, 1982.

[20] H. L. Bryden, and T. H. Kinder, "Steady two-layer exchange through the Strait of Gibraltar", *Deep-Sea Res.,* doi: 10.1016/S0198-0149(12)80020-3, 1991.

[21] M. Bormans, C. Garrett, and K. R. Thompson, "Seasonal variability of the surface inflow through the Strait of Gibraltar", *Oceanol. Acta*, vol. 9, 403-414, 1986.

[22] J. Candela, C. D. Winant, and H. L. Bryden, "Meteorologically forced subinertial flows through the Strait of Gibraltar" *J. Geophys. Res.*, doi: 10.1029/JC094iC09p12667, 1989.

[23] J. Candela, [Mediterranean Water and global circulation]. pp. 419-429 in Siedler, G., Church, J. and Gould, J. (eds.), [Ocean circulation and climate: observing and modelling the global ocean]. San Francisco, CA. USA: Academic Press, 736pp, (2001).

[24] J. García-Lafuente, J. M. Vargas, J. Delgado, and F. Criado, "Subinertial and seasonal variability in the Strait of Gibraltar from CANIGO observations" The 2nd Meeting on the Physical Oceanography of Sea Straits, Villefranche, 15th-19th April 2002. (2002).

[25] P. Brandt, A. Rubino, D. V. Sein, B. Baschek, A. Izquierdo, and J. O. Backhaus, "Sea level variation in the Western Mediterranean studied by a numerical tidal model of the Strait of Gibraltar", *J. Phys. Oceanogr.*, doi: 10.1175/1520-0485(2004)034<0433:SLVITW>2.0.CO;2, 2004.

[26] M. N. Tsimplis, and S. A. Josey, "Forcing of the Mediterranean Sea by atmospheric oscillations over the North Atlantic" *Geophys. Res. Lettr.* 28, 803-806, doi: 10.1029/2000GL012098, 2001.

[27] A. Cazenave, P. Bonnefond, F. Mercier, K. Dominh, and V. Toumazou, "Sea level variations in the Mediterranean Sea and Black Sea from satellite altimetry and tide gauges", *Global Planet. Change*, doi: 10.1016/S0921-8181(02)00106-6, 2002.

[28] T. Ross, C. Garrett, and P.-Y. Le Traon, "Western Mediterranean sea-level rise: Changing exchange flow through the Strait of Gibraltar" *Geophys. Res. Lettr.*, doi: 10.1029/2000GL011653, 2000.

[29] I. Fukumori, D. Menemenlis, and T. Lee, "A near-uniform basin-wide sea level fluctuation of the Mediterranean Sea", *J. Phys. Oceanogr.*, doi: 10.1175/JPO3016.1, 2007.

[30] C. J. R. Garrett, "Variable sea level and strait flows in the Mediterranean: A theoretical study of the response to meteorological forcing", *Oceanol. Acta*, vol. 6, 79-87, 1983.

[31] J. Candela, "The barotropic tide in the Strait of Gibraltar". In: *The Physical Oceanography of Sea Straits*, L.J. Pratt, Ed. The Netherlands: Kluwer Academic Publishers, doi: 10.1007/978-94-009-0677-8_22, pp. 457-475, 1990.

[32] R. Mañanes, M. Bruno, J. Alonso, B. Fraguela, and L. Tejedor, "Non-linear interaction between tidal and subinertial flows in the Strait of Gibraltar", *Oceanol. Acta*, vol 21, 33-46, 1998.

[33] L. Tejedor, A. Izquierdo, S. D. Sein, "Simulation of the semidiurnal tides in the Strait of Gibraltar", *J. Geophys. Res.*, doi: 10.1029/1998JC900102, 1999.

[34] G. Parrilla, S. Neuer, P.-Y. Le Traon, and E. Fernández, "Topical Studies in Oceanography: Canary Islands Azores Gibraltar Observations (CANIGO)". Vol. 2: studies of the Azores and Gibraltar regions, *Deep-Sea Res. PT II*, doi: 10.1016/S0967-0645(02)00136-4, 2002.

[35] A. Sánchez-Román, F. Criado-Aldeanueva, J. García-Lafuente, and J. C. Sánchez, "Vertical structure of tidal currents over Espartel and Camarinal sills, Strait of Gibraltar", *J. Marine Syst.*, doi: 10.1016/j.jmarsys.2007.11.007, 2008.

[36] L. Armi, and D. M. Farmer, "The flow of Mediterranean water through the Strait of Gibraltar", *Progr. Oceanogr.*, doi: 10.1016/0079-6611(88)90055-9, 1988.

[37] M. N. Tsimplis, "Vertical structure of tidal currents over the Camarinal Sill at the Strait of Gibraltar", *J. Geophys. Res.*, doi: 10.1029/2000JC900066, 2000.

[38] A. Izquierdo, L. Tejedor, D. V. Sein, O. Backhaus, P. Brandt, A. Rubino, and B. A. Kagan, "Control variability and internal bore evolution in the Strait of Gibraltar: a 2-D two-layer model study", *Estuar. Coast and Shelf S.*, doi: 10.1006/ecss.2000.0706, 2001.

[39] M. Bruno, J. J. Alonso, A. Cózar, J. Vidal, A. Ruiz-Cañavate, F. Echevarría, and J. Ruiz, "The boiling-water phenomena at Camarinal Sill, the Strait of Gibraltar", *Deep-Sea Res. PT II*, doi: 10.1016/S0967-0645(02)00144-3, 2002.

[40] O. Alvarez, C. J. Gonzalez, R. Mañanes, L. Lopez, M. Bruno, A. Izquierdo, J. Gómez-Enri, and M. Forero, "Analysis of short-period internal waves using wave-induced surface displacement: A 3D model approach in Algeciras Bay and the Strait of Gibraltar", *J. Geophys. Res.-Oceans*, doi: 10.1029/2011JC007393, 2011.

[41] D. Menemenlis, I. Fukumori, and T. Lee, "Atlantic to Mediterranean Sea Level Difference Driven by Winds near Gibraltar Strait", *J. Phys. Oceanogr.*, doi: 10.1175/JPO3015.1, 2007.

[42] J. Gómez-Enri, P. Villares, B. Tejedor, A. Aboitiz, I. Laiz, J. Coca, S. Vignudelli, P. Cipollini, M. Passaro and J. R. Torres, "From ENVISAT RA-2 to CRYOSAT SIRAL: validation of altimeter products near the coast (the ALCOVA Project)". Proc. SPIE 9240, Remote Sensing of the Ocean, Sea Ice, Coastal Waters, and Large Water Regions 2014, 92400P (14 October 2014); doi: 10.1117/12.2067501, 2014.

[43] L. Roblou, F. Lyard, M. Le Henaff, and C. Maraldi, "X-TRACK, a new processing tool for altimetry in coastal oceans". IEEE Geoscience and Remote Sensing Symposium, Barcelona, Spain, (23–27 July 2007) (pp. 5129–5133). IEEE, 2007.

[44] L. Roblou, J. Lamouroux, J. Bouffard, F. Lyard, M. Le Hénaff, A. Lombard, P. Marsalaix, P. De Mey, and F. Birol, "Post-processing altimeter data toward coastal applications and integration into coastal models". In: Vignudelli, S., Kostianoy, A., Cipollini, P., Benveniste, J. (Eds.), *Coastal Altimetry*. Berlin, Germany: Springer-Verlag, pp. 217-246, 2011.

[45] IOC "Global Sea Level Observing System (GLOSS). Implementation Plan 1997". Intergovernamental Oceananographyc Commission. Technical Series 50:91 & Annexes. 1997

[46] European Sea-level Observing Systems (EOSS). "Status and Future Developments. Cost Action 40". ISBN: 92-894-0310-1. 2000.

[47] M. García, B. Pérez, and M. A. Fraile, "Sea Level Observing Activities. Spanish national report for GLOSS". Paris, 5 June 2007.

[48] Y. Cheng, and O. B. Andersen, "Multimission empirical ocean tide modelling for shallow waters and polar seas", *J. Geophys. Res.-Oceans*, doi: 10.1029/2011JC007172, 2011.

[49] F. Lyard, F. Lefèvre, T. Letellier and O. Francis, "Modelling the global ocean tides: modern insights from FES2004", *Ocean Dynamics*, doi: 10.1007/s10236-006-0086-x, 2006

[50] F. M. Calafat, D. P. Chambers, and M. N. Tsimplis, "Mechanisms of decadal sea level variability in the eastern North Atlantic and the Mediterranean Sea", *J. Geophys. Res.-Oceans*, doi: 10.1029/2012JC008285, 2012.

[51] S. A. R. Sultan, F. Ahmad, N. M. Elghribi, and A. M. Al-Subhi, "An analysis of Arabian Gulf monthly mean sea level", *Cont. Shelf Res.*, doi: 10.1016/0278-4343(94)00081-W, 1995.

[52] F. Oreiro, E., D'Onofrio, W. Grismeyer, M. Fiore, M. Saraceno, "Comparison of tide model outputs for the northern region of the Antarctic Peninsula using satellite altimeters and tide gauge data", *Polar Sci.*, doi: 10.1016/j.polar.2013.12.001, 2014.

[53] L. Carrère, and F. Lyard, "Modeling the barotropic response of the global ocean to atmospheric wind and pressure forcing - comparisons with observations". *Geophys. Res. Lett.*, doi: 10.1029/2002GL016473, 2003.

[54] O. B. Andersen, and P. Knudsen, "The DNSC08 mean sea surface and mean dynamic topography". *J. Geophys. Res.-Oceans*, doi: 10.1029/2008JC005179, 2009.

[55] O. B. Andersen, "The DTU10 Gravity field and Mean sea surface", Second international symposium of the gravity field of the Earth (IGFS2), Fairbanks, Alaska, 2010.

[56] S. Labroue, "RA2 ocean and *MWR* measurement long term monitoring, 2007 report for WP3, Task 2 - *SSB* estimation for RA2 altimeter", Contract 17293/03/I-OL. *CLS*-DOS-NT-07-198, 53pp. *CLS* Ramonville St. Agne, 2007.

[57] S. Abdalla, "Ku-band radar altimeter surface wind speed algorithm", *Mar. Geod.*, doi: 10.1080/01490419.2012.718676, 2012.

[58] K.-H. Tseng, C. K. Shum, Y. Yi, W. J. Emery, C-Y Kuo, H. Lee, and H. Wang, "The improved retrieval of coastal sea surface heights by retracking modified radar

altimeter waveforms", *IEEE T. Geosci. Remote.*, doi: 10.1109/TGRS.2013.2246572, 2013.

[59] N. H. Idris, X. Deng, and O. B. Andersen, "The Importance of coastal altimetry retracking and detiding: a case study around the Great Barrier Reef, Australia", *Int. J. Remote Sens.*, doi: 01431161.2014.882032, 2014.

[60] K.-H. Tseng, C. K. Shum, Y. Yi, H. S. Fok, C.-Y. Kuo, H. Lee, X. Cheng, and X. Wang, "Envisat altimetry radar waveform retracking of quasi-specular echoes over the ice-covered Qinghai Lake", *Terr. Atmos. Ocean Sci.*, doi: 10.3319/TAO.2012.12.03.01(TibXS), 2013.

[61] H. Snaith, P. Cipollini, L. West, "Development of Radar Altimetry Data Processing in the Oceanic Coastal Zone". EWP1 – Deliverable D1.1. Product Specification Document. ESA/ESRIN Contract No. 21201/08/I-LG. 2011.

[62] J. Bouffard, L. Roblou, F. Birol, A. Pascual, L. Fenoglio-Marc, M. Cancet, R. Morrow, and Y. Ménard, "Introduction and assessment of improved coastal altimetry strategies: Case study over the Northwestern Mediterranean Sea". In: Vignudelli, S., Kostianoy, A., Cipollini, P., Benveniste, J. (Eds.), *Coastal Altimetry*. Berlin, Germany: Springer-Verlag, pp. 297-330, 2011.

TABLE 1

Table 1. Along-track mean *rmse* (in cm) in the two track segments analyzed (D#0360 and A#0831) with different land masks applied to the Envisat RA-2 18-Hz data. The number of valid data used to estimate the mean *rmse* is shown in parenthesis.

	D#0360 (*E-SoG*)		**A#0831** (*W-SoG*)	
	ALES	SGDR	ALES	SGDR
No land mask applied	14.4 (49)	17.0 (49)	12.1 (67)	16.6 (67)
Land mask: 1 km	13.6 (42)	15.9 (42)	11.8 (63)	16.2 (63)
Land mask: 2 km	13.4 (36)	15.7 (36)	11.8 (60)	15.4 (60)
Land mask: 3 km	13.4 (31)	15.9 (31)	11.7 (57)	15.3 (57)
Land mask: 4 km	13.3 (26)	15.4 (26)	11.7 (55)	15.3 (55)
Land mask: 5 km	13.5 (20)	15.4 (20)	11.7 (49)	15.3 (49)

FIGURE CAPTIONS

Figure 1. Study area: the Strait of Gibraltar located between Africa and Europe. Also included are the position of the tide gauges and the location of the two passes analyzed: Ascending pass #0831 and descending pass #0360. The length of the 'ocean' track segments used and the distance to the tide gauge are also included.

Figure 2. Sea level (in m) recorded by tide gauge: *Tarifa_ENV* at 5-minutes interval during the Envisat time period (October 2002 - October 2010). Data are referred to the Tide Gauge Zero. Fig. 2.b: zoom-in of the water level between May and July 2007.

Figure 3. Envisat RA-2 radargrams of along-track waveform power for descending D#0360 (3.a) and ascending A#0831 (3.c) track segments with the chirp bandwidth also included. The selected cycle was number 73 in both cases. The along-track SLA profiles (useful data) are shown in Fig. 3.b (D#0360) and 3.d (A#0831). Red arrow indicates the segments with rejected data after screening. The big black arrows give the latitudinal position of the tide gauge.

Figure 4. Envisat data availability (# of cycles) along the two tracks analyzed: D#0360 (4.a) and A#0831 (4.b). Grey dashed line gives the maximum number of cycles: 66 (D#0360) and 74 (A#0831). Black solid line indicates the number of cycles after applying the chirp_id mask to the dataset. Green solid line gives the number of along-track cycles used to estimate SLA after applying the editing of the corrections. Red solid line shows the number of cycles after all the outliers in SLA were removed. The big black arrows give the latitudinal position of the tide gauge.

Figure 5. Time series of in-situ SLA (Fig. 5.a and 5.c) and altimeter-derived SLA: SGDR (blue line) and ALES (red line) (Fig. 5.b and 5.d) for descending pass #0360 and ascending pass #0831, respectively. The 18-Hz position selected was at the lowest *rmse* found at both ALES and SGDR datasets along the entire track segments.

Figure 6. *rmse* along the two track segments analyzed: D#0360 (Fig. 6.a) and A#0831 (Fig. 6.b). Blue lines show the results obtained with Envisat SGDR and red lines those from Envisat ALES. Black dots are the *rmse* for CTOH Envisat dataset (1 Hz). Also included the *rmse* from AltiKa/standard (pink line) and AltiKa/ALES (brown line).

FIGURE 1

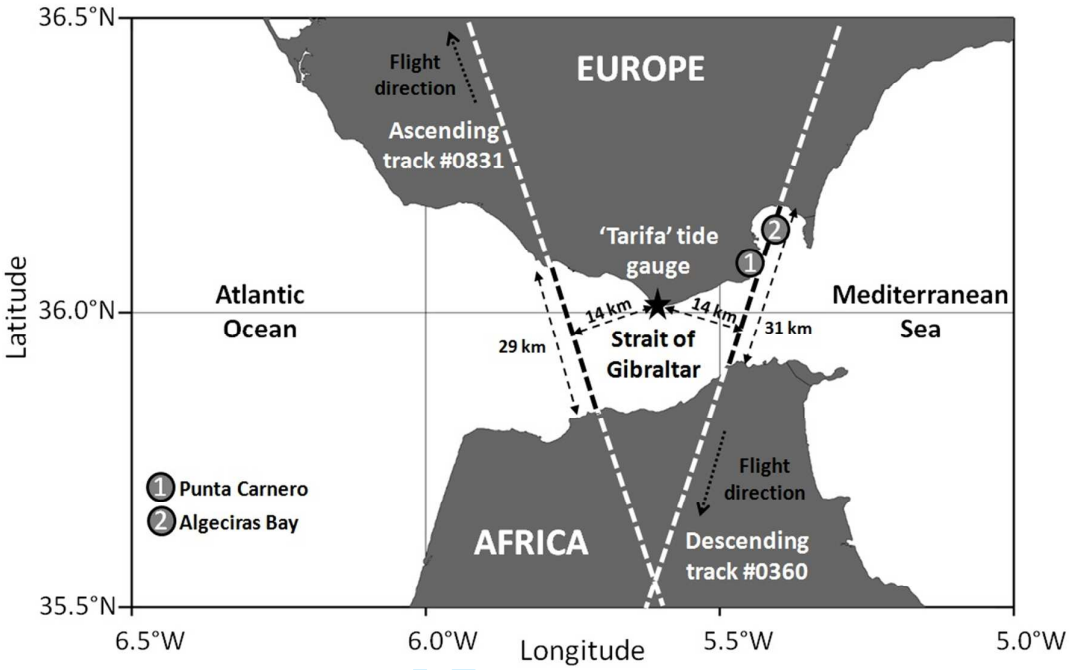

Figure 1. Study area: the Strait of Gibraltar located between Africa and Europe. Also included are the position of the tide gauges and the location of the two passes analyzed: Ascending pass #0831 and descending pass #0360. The length of the 'ocean' track segments used and the distance to the tide gauge are also included.

FIGURE 2

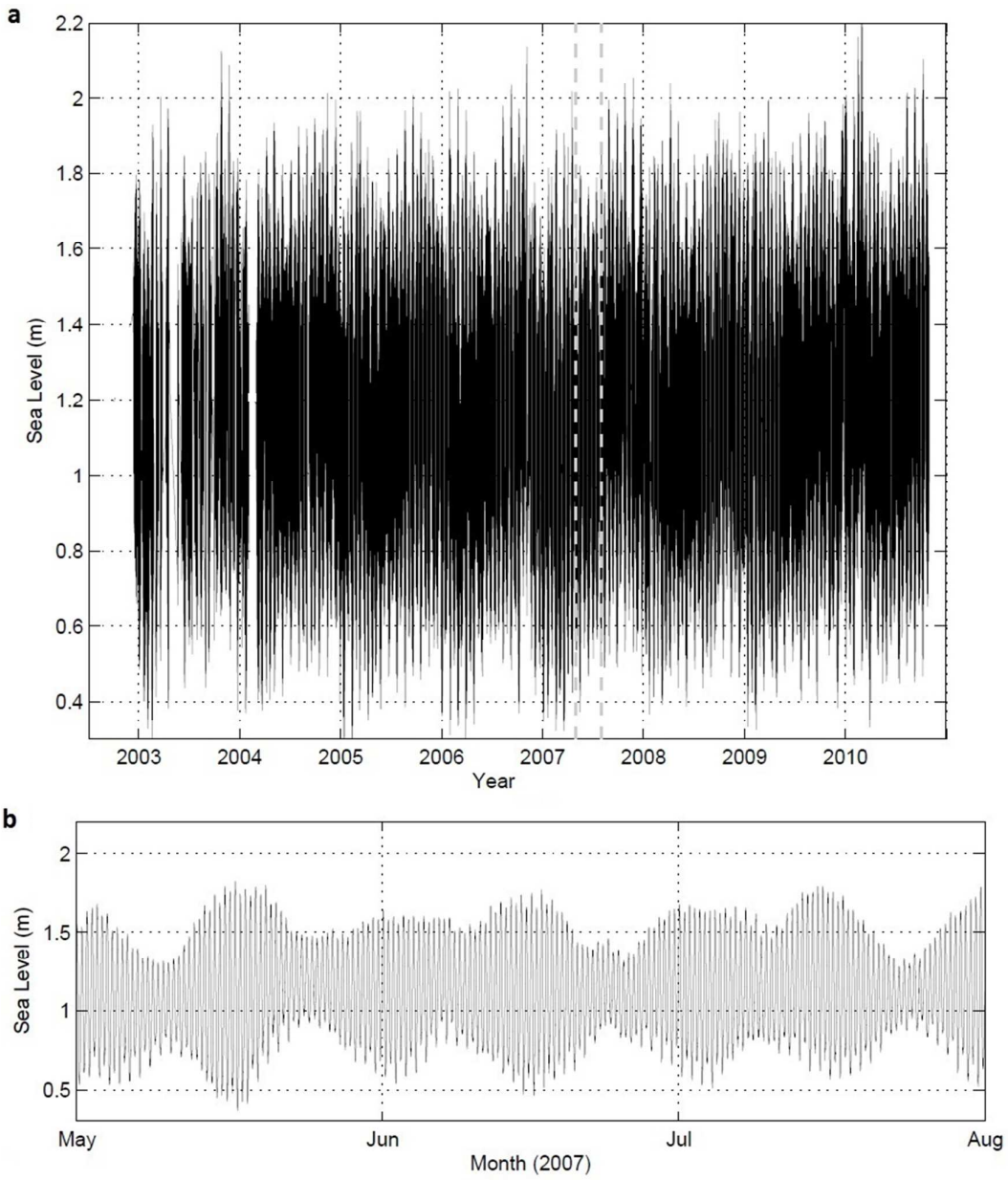

Figure 2. Sea level (in m) recorded by tide gauge: *Tarifa_ENV* at 5-minutes interval during the Envisat time period (October 2002 - October 2010). Data are referred to the Tide Gauge Zero. Fig. 2.b: zoom-in of the water level between May and July 2007.

FIGURE 3

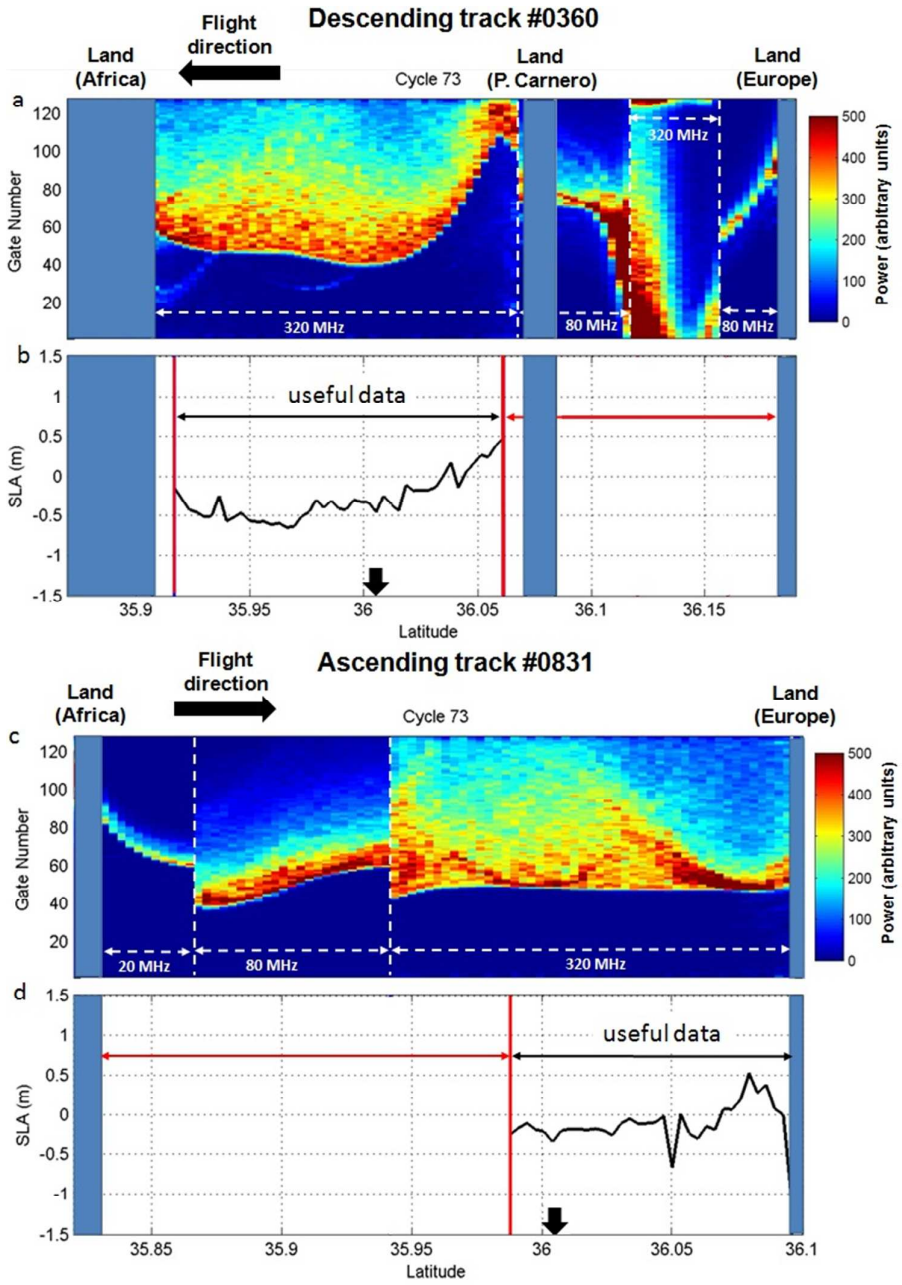

Figure 3. Envisat RA-2 radargrams of along-track waveform power for descending D#0360 (3.a) and ascending A#0831 (3.c) track segments with the chirp bandwidth also included. The selected cycle was number 73 in both cases. The along-track SLA profiles (useful data) are shown in Fig. 3.b (D#0360) and 3.d (A#0831). Red arrow indicates the segments with rejected data after screening. The big black arrows give the latitudinal position of the tide gauge.

FIGURE 4

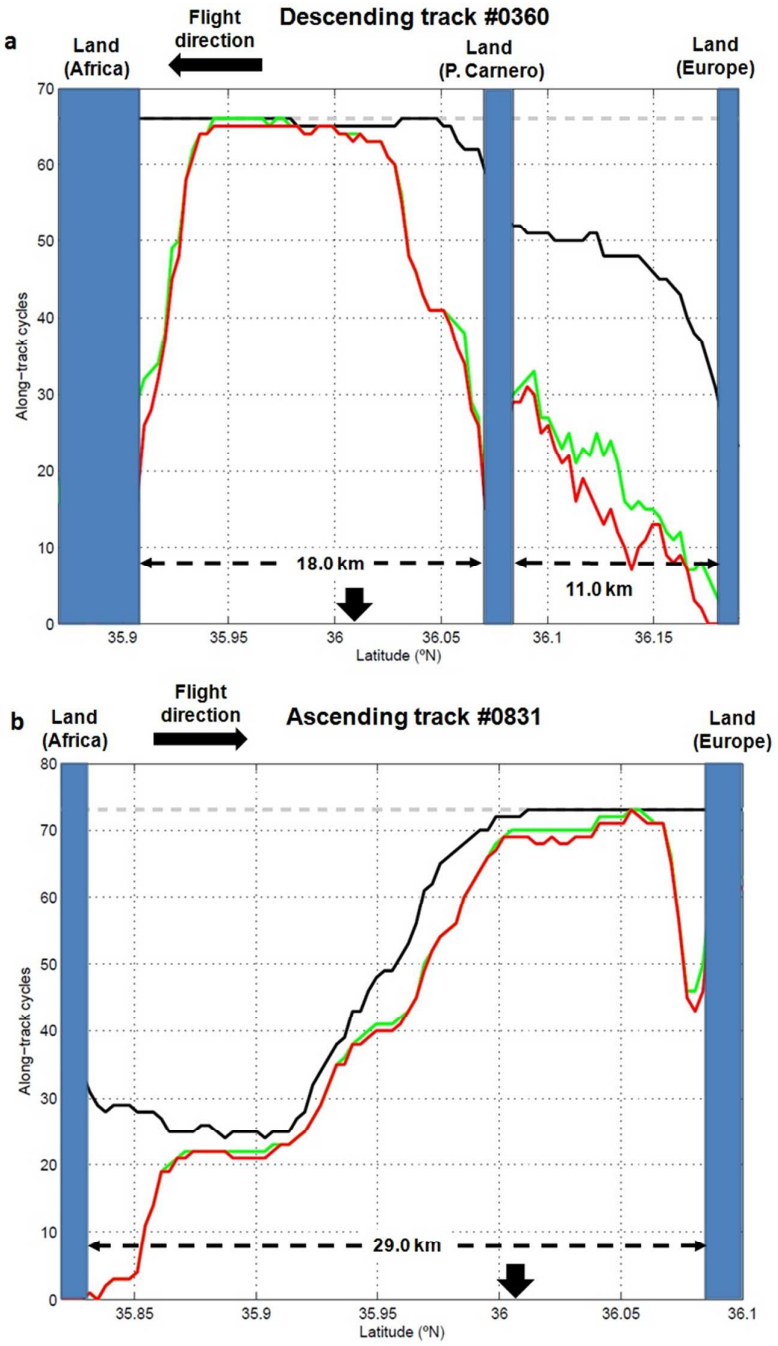

Figure 4. Envisat data availability (# of cycles) along the two tracks analyzed: D#0360 (4.a) and A#0831 (4.b). Grey dashed line gives the maximum number of cycles: 66 (D#0360) and 74 (A#0831). Black solid line indicates the number of cycles after applying the chirp_id mask to the dataset. Green solid line gives the number of along-track cycles used to estimate SLA after applying the editing of the corrections. Red solid line shows the number of cycles after all the outliers in SLA were removed. The big black arrows give the latitudinal position of the tide gauge.

FIGURE 5

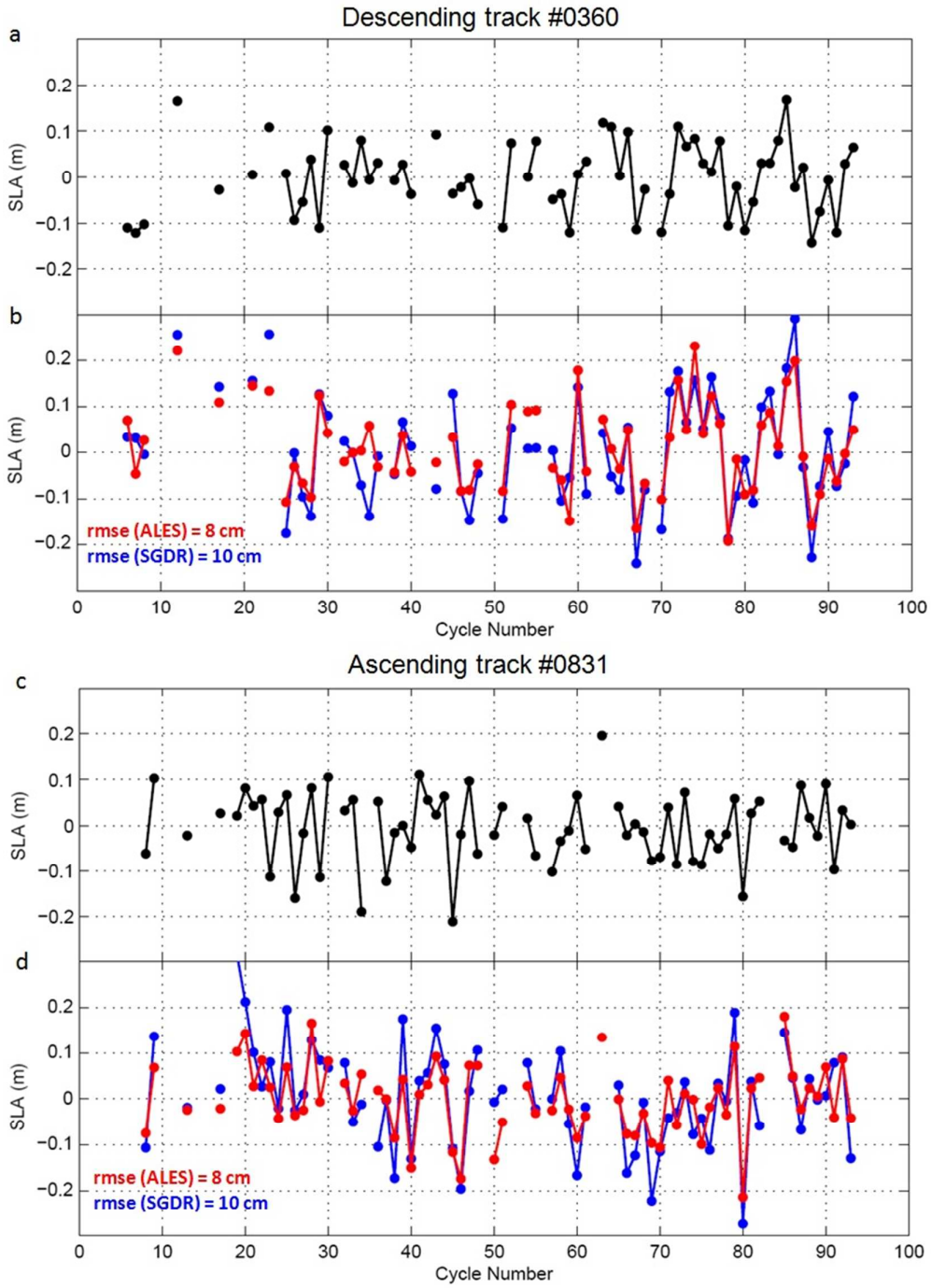

Figure 5. Time series of in-situ SLA (Fig. 5.a and 5.c) and altimeter-derived SLA: SGDR (blue line) and ALES (red line) (Fig. 5.b and 5.d) for descending pass #0360 and ascending pass #0831, respectively. The 18-Hz position selected was at the lowest *rmse* found at both ALES and SGDR datasets along the entire track segments.

FIGURE 6

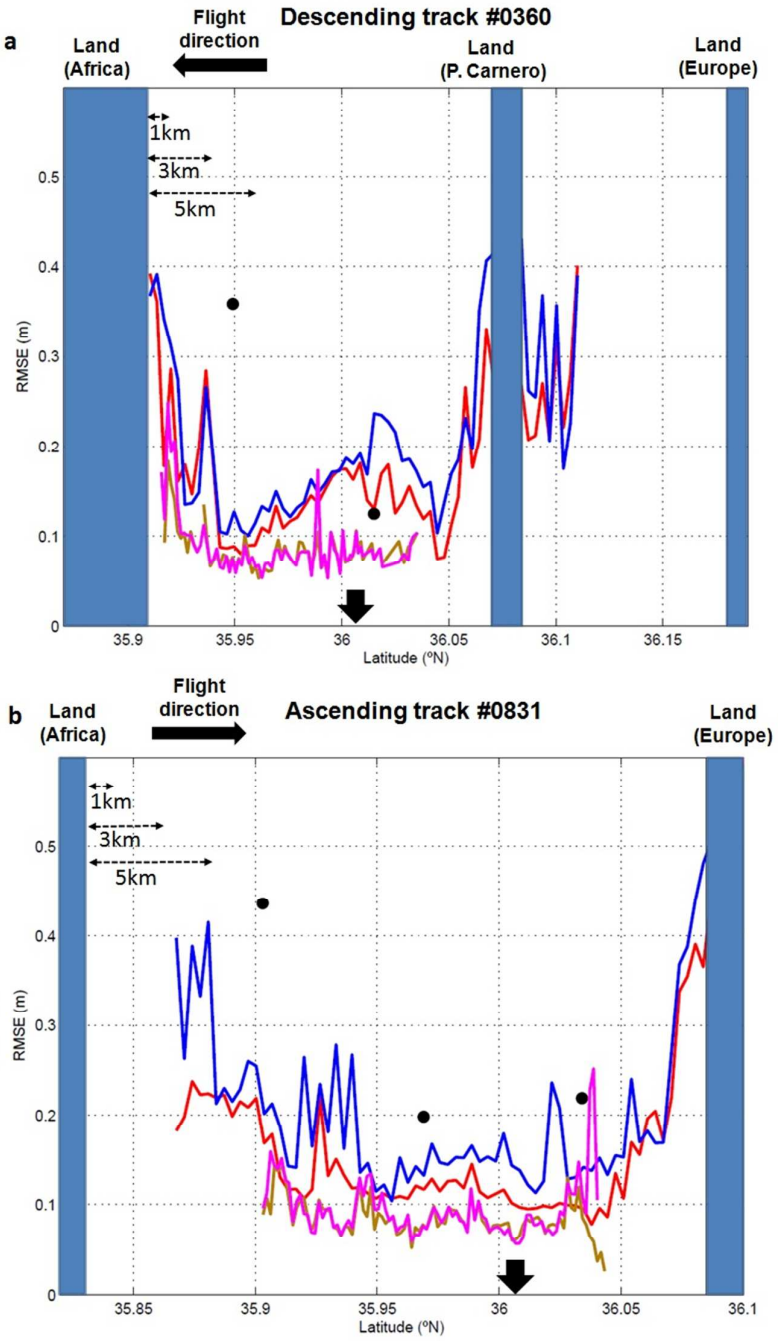

Figure 6. *rmse* along the two track segments analyzed: D#0360 (Fig. 6.a) and A#0831 (Fig. 6.b). Blue lines show the results obtained with Envisat SGDR and red lines those from Envisat ALES. Black dots are the *rmse* for CTOH Envisat dataset (1 Hz). Also included the *rmse* from AltiKa/standard (pink line) and AltiKa/ALES (brown line).